

Dear Heini,

Thanks a lot for your comments and for acceptance of the paper. We made the necessary corrections and explained the remaining unclear points:

line 36 and line 103: striking --> strikingly

no, we meant striking anomalies, not strikingly different anomalies.

line 64: state --> stated

done

line 67 and in many other places: references should be in chronological order!

We checked that and made changes accordingly.

line 105: reports --> reported

done

line 117: Lorius --> Lorius et al.

done

line 143: explain what AWS means

done

line 174: I still find this statement at least surprising: 500 hPa seems to me a rather high level for strong moisture transport (I expect it to be at lower levels, e.g., 800 hPa). Obviously you claim the opposite that other studies assumed the transport of moisture to occur at higher levels ... can you give references for this?

In the Dittmann et al. paper, trajectories were calculated for arrival levels 600hPa, 500hPa and 300hPa. Since Dome Fuji is situated at an elevation, where even the 600hPa trajectory can (and does) disappear in the snow sometimes, it is not possible to calculate a trajectory for an arrival level lower than 600hPa. The 600hPa trajectories often showed a rather local path and could not be used to explain the moisture transport for the precipitation events. The 500hPa-arrival level trajectory, of course, had starting points (end points of the back-trajectory) way lower than 500hPa, often enough close to the surface (thankgod, because we assumed evaporation from the ocean somewhere close to that point in many cases. Sometimes the moisture source was even further north, and then the trajectory did not reach yet levels close to the surface after 5 days). The three-dimensional moisture transport is still not fully understood yet (particularly in the escarpment areas), but the picture we have now is, that usually in the cases of event-type precipitation, warm and moist air is advected southward in a rather thick layer, starting close to the surface and reaching up higher than 500hPa, and then orographically lifted. So, of course, it is too simple and not correct to say the transport takes place mainly at the 500hPa level. Only the trajectory with 500hPa arrival level seemed to be the most representative for the general moisture transport to Dome F. In ice core papers, often a different height of moisture transport was given as explanation for different findings for e.g. deuterium excess at different altitude ranges (with a rather arbitrary threshold at 1500m, sometimes 2000m). Rather vague without a physical explanation. From earlier models a moisture origin between 20° and 30°

South was stated, also without any explanation of the mechanisms that transported the moisture from the subtropics to Antarctica and about the precipitation mechanisms. We found that the orographic lifting is essential for precipitation in the interior of the continent, since there are no frontal systems with dynamical lifting of the air masses.

Since this is all quite complex and we removed the trajectory calculations from this paper, we simply removed the parts in brackets in the final version and keep the discussion for a future paper. We think, that, for the present study, it would distract too much from the main points. We also added a reference (Masson-Delmotte et al. 2008 and references therein), a review paper, in which these things are discussed.

line 279: I don't understand the intention of the sentence: "... precipitation ... on 9 Feb ... followed by ... on 10 Feb ... stems from one event around 9 Feb" - this seems to be obvious to me, what is really the point?

We deleted that sentence.

line 362/364: I think the word "composite" is confusing here, you just calculated the monthly mean(?)

We agree and changed this to "mean".

line 460: state --> stated

done

line 516: now --> snow

done

Yours sincerely / best regards

Elisabeth Schlosser

1 **Precipitation and synoptic regime in two extreme years**
2 **2009 and 2010 at Dome C, Antarctica – implications for ice**
3 **core interpretation**

4
5
6 **E. Schlosser^{1,2}, B. Stenni³, M. Valt⁴, A. Cagnati⁴, J. G. Powers⁵, K. W. Manning⁵,**
7 **M. Raphael⁶, and M. G. Duda⁵**

8
9 [1] {Inst. of Atmospheric and Cryospheric Sciences, University of Innsbruck,
10 Innsbruck, Austria}

11 [2] {Austrian Polar Research Institute, Vienna, Austria}

12 [3] {University of Venice, Venice, Italy}

13 [4] {Avalanche Service Arabba, Italy}

14 [5] {National Center for Atmospheric Research, Boulder, CO, USA}

15 [6] {Department of Geography, University of California, Los Angeles, California,
16 USA}

17

18

19

20

21

submitted to: Atmospheric Chemistry and Physics

22

18 September 2015

23

revised version for ACPD 13 October 2015

24

revised version after review 10 February 2016

25

re-revised version March 23th 2016

26

▲ final version April 7th 2016 ▲▲

27

28 Correspondence to: E. Schlosser (Elisabeth.Schlosser@uibk.ac.at)

29

Formatiert: Schriftart: (Standard)
Times New Roman, 12 Pt.

Formatiert: Schriftart: (Standard)
Times New Roman, 12 Pt., Hochgestellt

Formatiert: Schriftart: (Standard)
Times New Roman, 12 Pt.

30

31 **Abstract**

32

33 At the East Antarctic deep ice core drilling site Dome C, daily precipitation measurements
34 have been initiated in 2006 and are being continued until today. The amounts and stable
35 isotope ratios of the precipitation samples as well as crystal types are determined. Within the
36 measuring period, the two years 2009 and 2010 showed striking contrasting temperature and
37 precipitation anomalies, particularly in the winter seasons. The reasons for these anomalies
38 are analysed using data from the mesoscale atmospheric model WRF (Weather Research and
39 Forecasting Model) run under the Antarctic Mesoscale Prediction System (AMPS). 2009 was
40 relatively warm and moist due to frequent warm air intrusions connected to amplification of
41 Rossby waves in the circumpolar westerlies, whereas the winter of 2010 was extremely dry
42 and cold. It is shown that while in 2010 a strong zonal atmospheric flow was dominant, in
43 2009 an enhanced meridional flow prevailed, which increased the meridional transport of heat
44 and moisture onto the East Antarctic plateau and led to a number of high-
45 precipitation/warming events at Dome C. This was also evident in a positive (negative) SAM
46 (Southern Annular Mode) index and a negative (positive) ZW3 (Zonal Wave number three)
47 index during the winter months of 2010 (2009). Changes in the frequency or seasonality of
48 such event-type precipitation can lead to a strong bias in the air temperature derived from
49 stable water isotopes in ice cores.

50

51

52 **1 Introduction**

53

54 Although Antarctic precipitation has been studied for approximately half a century (see e.g.
55 Bromwich, 1988), a number of open questions remain. There are two key motivations for
56 studying Antarctic precipitation. The first is that precipitation/snowfall is the most important
57 positive component of the mass balance of Antarctica. This is receiving increasing attention in
58 discussions of climate change since the mass balance response to global warming can
59 considerably influence sea level change. A possible increase of precipitation in a future
60 climate due to higher air temperatures and therefore increased saturation vapour pressure
61 would mean storage of larger amounts of water in the Antarctic ice sheet, thus mitigating sea

62 level rise (Church et al., 2013). So far, the expected increase in precipitation has not been
63 found in the measurements (e.g. Monaghan et al., 2006). However, in one projection derived
64 from a combination of various models and ice core data, Frieler et al. (2015) stated a possible
65 increase in Antarctic accumulation on the continental scale of approximately 5% K⁻¹. In some
66 parts of Antarctica, higher accumulation would lead to increased ice flow and thus dynamical
67 ice loss, which would reduce the total mass gain (Winkelmann et al., 2012; Harig and Simons,
68 2015; ~~Winkelmann et al., 2012~~). Thus, for modelling and calculation of the Antarctic mass
69 balance, precipitation amounts and precipitation regimes have to be known as exactly as
70 possible.

71 A second driver for studying Antarctic precipitation is that the ice of Antarctica is an
72 unparalleled climate archive: ice cores up to 800.000 years old yield crucial information about
73 palaeotemperatures and the past constitution of the atmosphere (e.g. EPICA community
74 members, 2004). To derive former air temperatures from ice cores, the stable-isotope ratios of
75 water are used primarily. A linear spatial relationship has been found between mean annual
76 stable isotope ratios in Antarctic precipitation and annual mean air temperature at the
77 deposition site although the isotope ratios depend in a complex way on mass-dependent
78 fractionation processes during moisture transport and precipitation formation (Dansgaard,
79 1964). This spatially derived linear relationship has been found not to hold temporally,
80 however (Jouzel et al., 2003; Jouzel, 2014). Apart from air temperature, several other factors
81 influence the stable isotope ratio, such as seasonality of precipitation, location of and
82 conditions at the moisture sources and conditions along moisture transport paths (e.g. Noone
83 et al., 1999; Schlosser, 1999; Jouzel et al., 2003; Sodemann et al., 2008; Sodemann and Stohl,
84 2009; ~~Sodemann et al., 2008, Jouzel et al., 2003; Noone et al., 1999; Schlosser, 1999~~). Thus,
85 for a correct interpretation of the ice core data a thorough understanding of the atmospheric
86 processes responsible for the precipitation is needed, as it was the precipitation that ultimately
87 formed the glacier ice investigated in the cores. In particular, information about precipitation
88 mechanisms, moisture sources and transport paths, and atmospheric conditions at the final
89 deposition site is required.

90 Measuring Antarctic precipitation is a challenge, not only due to the remoteness and extreme
91 climate of the continent, but also due to difficulties in distinguishing between drifting/blowing
92 snow and falling precipitation. The latter is due to the high wind speeds that typically
93 accompany precipitation events in coastal areas. In the interior of the continent, while wind
94 speeds are lower than at the coast, the threshold for drifting snow is often lower due to lower

95 snow densities as well. Measurements are also complicated by the extremely small amounts
96 of precipitation produced in the cold and dry air. Precipitation measurements with optical
97 devices may hold some hope for improved data in the future, but these instruments are
98 currently in the testing phase in Antarctica (Colwell, pers. comm.). In light of the lack of
99 observations, atmospheric models have become increasingly useful tools to investigate
100 Antarctic precipitation (Noone and Simmons, 1998; Noone et al., 1999; Noone and Simmons,
101 2002; Bromwich et al., 2004; Schlosser et al., 2008, 2010a; 2010b; 2008; ~~Noone and~~
102 ~~Simmons, 2002; Noone et al., 1999; Noone and Simmons, 1998~~).

103 This study focusses on the differences in the precipitation regime of two contrasting years
104 within the short measuring period, motivated by the consequences different precipitation/flow
105 regimes have on stable isotope interpretation. The present investigation concentrates on the
106 years 2009 and 2010. These years were chosen because they showed striking contrasting
107 temperature and precipitation anomalies, particularly in the winter seasons. Fogt (2010)
108 reported that temperatures in the Antarctic were persistently above average in the mid-to-
109 lower troposphere during the winter of 2009. The positive surface temperature anomalies
110 were most marked in East Antarctica. In 2010, the picture was very different from 2009, with
111 generally below-average temperatures on the East Antarctic plateau in winter and spring
112 (Fogt, 2011).

113

114

115 **2 Study site**

116 Dome C (75.106 °S, 123.346 °E, elevation 3233m) is one of the major domes on the East
117 Antarctic ice sheet. Its mean annual temperature is -54.5 °C, and the mean annual
118 accumulation derived from ice cores amounts to 25 mm water equivalent (w.e.)/yr. Several
119 deep ice cores have been retrieved at Dome C, the first one in 1977/78, reaching a depth of
120 906 m, corresponding to an age of approximately 32,000 yr. The thermally drilled core was
121 retrieved during the International Antarctic Glaciological Project (Lorius et al., 1979).

122 The oldest ice to date has been obtained at Dome C through the European deep drilling
123 project EPICA (European Project for Ice Coring in Antarctica). The drilling was completed in
124 January 2006; at the base of the 2774.15 m long ice core the age of the ice was estimated to be
125 800,000 yr, thus covering eight glacial cycles (EPICA community members, 2004). To

126 support the EPICA drilling operation, the French-Italian Antarctic wintering base Dome
127 Concordia became operational in 2005.

128

129

130 **3 Previous work**

131 Precipitation conditions in the interior of Antarctica are very different from those in coastal
132 areas. Whereas precipitation at the coast is usually caused by frontal systems of passing
133 cyclones that form in the circumpolar trough (e.g. Simmonds et al., 2002), in the interior
134 different precipitation mechanisms are at play. On the majority of days, only diamond dust,
135 also called clear-sky precipitation, is observed. It forms due to radiative cooling in a nearly
136 saturated air mass. Although diamond dust is predominant temporally, it does not necessarily
137 account for the largest fraction of the total yearly precipitation. It has been shown that a few
138 snowfall events per year can bring up to 50% of the total annual precipitation (Braaten et al.,
139 2000; Reijmer and van den Broeke, 2003; Fujita and Abe, 2006; Schlosser et al., 2010a;
140 Gorodetskaya et al., 2013). Those events are due to amplification of Rossby waves in the
141 circumpolar westerlies, which increases the meridional transport of heat and moisture
142 polewards. In extreme cases this can even mean a transport from the Atlantic sector across the
143 continent to the Pacific side (Sinclair, 1981; Schlosser et al., 2015b) The relatively moist and
144 warm air is orographically lifted over the ice sheet, followed by cloud formation and/or
145 precipitation (Noone et al, 1999; Massom et al., 2004; Birnbaum et al., 2006; Schlosser et al.,
146 2010). Except for the study by Fujita and Abe (2006), all of these investigations were based
147 on model and **Automatic Weather Station (AWS)** data, rather than daily precipitation
148 measurements.

149 For a long time it was believed in ice core studies that precipitation represented in Antarctic
150 ice cores is formed close to the upper boundary of the temperature inversion layer assuming
151 that the largest moisture amounts are found where the air temperature is highest (Jouzel and
152 Merlivat, 1984). This is a very simplified view that is, however, widely used in ice core
153 studies. It assumes that there are basically no multiple temperature inversions and that
154 humidity is only dependent on temperature through the Clausius-Clapeyron equation, which
155 describes the temperature dependence of vapour pressure. This would mean that humidity and
156 temperature inversions would always have a similar profile. However, more recent studies
157 have shown that humidity inversions are parallel to the temperature inversion only in 50% of

158 the cases, and often multiple humidity (and temperature) inversions occur (Nygard et al.,
159 2013). In particular, the local cycle of sublimation and re-sublimation (deposition) is poorly
160 known, but it is important for both mass balance and isotope fractionation studies.

161 At Dome Fuji, at an elevation of 3810m, the air can be so dry that, in spite of the advection of
162 warm and moist air related to amplified Rossby waves, no precipitation is observed at the site.
163 However, this synoptic situation can cause a strong warming in the lower boundary layer
164 (particularly during blocking situations) due to a combination of warm air advection and
165 removal of the temperature inversion layer by increased wind speed that induces mixing and
166 cloud formation, which in turn increases downwelling longwave radiation (Enomoto et al,
167 1998; Hirasawa et al., 2000). Increased precipitation amounts can also be observed after a
168 snowfall event when the warm air advection has ended, but increased levels of moisture
169 prevail, which can lead to extraordinarily high amounts of diamond dust precipitation
170 (Hirasawa et al., 2013). In West Antarctica, intrusions of warm, marine air can lead to
171 increased cloudiness, precipitation and air temperature. A change in the frequency or intensity
172 of such warm air intrusions could have a large effect on West Antarctic climate if the mean
173 general circulation changed (Nicolas and Bromwich, 2011).

174 Moisture origin has been investigated in various studies using back-trajectory calculations
175 employing different models and methods (Reijmer et al., 2002; Sodemann et al. 2008; Suzuki
176 et al., 2008; Sodemann and Stohl, 2009; Scarcilli et al., 2010; ~~Sodemann and Stohl, 2009;~~
177 ~~Sodemann et al. 2008; Suzuki et al., 2008; Reijmer et al., 2002~~). In a recent study by
178 Dittmann et al. (2015), who investigated precipitation and moisture sources at Dome F for
179 precipitation events in 2003, it was estimated that the origin of the moisture was farther south
180 (on average at 50°S) and the transport occurred lower in the atmosphere (~~approximately at the~~
181 ~~500 hPa level~~) than previously assumed in ice core studies (Masson-Delmotte et al., 2008).

182 Dome C is a deep ice core drilling site. However, the measurements presented here are the
183 first derived from fresh snow samples at this site. A similar study, if only for a period of
184 approximately one year, was carried out by Fujita and Abe (2006) at Dome Fuji (see Fig. 1),
185 another deep-drilling site in East Antarctica. They investigated daily precipitation data
186 together with measurements of stable isotope ratios of the precipitation samples. Temporal
187 variations of $\delta^{18}\text{O}$ were highly correlated with air temperature. Half of the annual
188 precipitation resulted from only 11 events (18 days), without showing any seasonality. The
189 other half was due to diamond dust. Similar results were found in studies by Schlosser et al.
190 (2010a), at Kohnen Station (see Fig. 1) and by Reijmer and Van den Broeke (2003), who used

191 data from automatic weather stations in Dronning Maud Land. The precipitation-weighted
192 temperature was significantly higher than the mean annual surface temperature because the
193 precipitation events were related to warm-air advection, which leads to a warm bias in the
194 $\delta^{18}\text{O}$ record.

195

196 **4 Data and methods**

197 **4.1 Precipitation**

198 Daily precipitation measurements were initiated at Dome C in 2006, and have, with some
199 interruptions, been continued until today. Daily precipitation amounts are measured using a
200 wooden platform set up at a distance of 800 m from the main station, at a height of 1 m above
201 the snow surface to avoid contributions from low drifting snow. For the same reason, the
202 platform is surrounded by a rail of approximately 8 cm height. The measurements include
203 precipitation sampling and analysis of stable water isotopes ($\delta^{18}\text{O}$, δD) of the samples.
204 Additionally, the crystal structure of the precipitation is analysed in order to distinguish
205 between diamond dust, snowfall, and drift snow. Diamond dust consists of extremely fine ice
206 needles whereas synoptic snowfall shows various types of regular snow crystals, which tend
207 to be broken in case of drifting/blowing snow. The snow crystal type depends on air
208 temperature during formation in the cloud. Samples of mixed crystal types can also occur.

209 While errors of the precipitation measurements cannot be quantified, it is understood that they
210 can exceed 100% given the extremely small precipitation amounts.

211 The Dome C precipitation series is the first and so far only multi-year precipitation/stable
212 isotope series at an Antarctic deep ice core drilling site.

213

214 **4.2 AWS data**

215 The Antarctic Meteorological Research Center (AMRC) and Automatic Weather Station
216 (AWS) Program are sister projects of the University of Wisconsin-Madison funded under the
217 United States Antarctic Program (USAP) that focus on data for Antarctic research support,
218 providing real-time and archived weather observations and satellite measurements and
219 supporting a network of automatic weather stations across Antarctica.

220 The current AWS at Dome C was set up by the AMRC, in December 1995. The station
221 measures the standard meteorological variables of air temperature, pressure, wind speed, wind
222 direction, and humidity. Data can be obtained from <http://amrc.ssec.wisc.edu>. Note that an
223 initial AWS (named Dome C) had been set up in 1985, however, at a distance of about 70 km
224 from the current site. Thus, only data from the new station (Dome C II) are used in the present
225 study.

226

227 4.3 WRF Model Output from the AMPS Archive

228 In addition to the observations described above, this study uses numerical weather prediction
229 (NWP) model output for analysis of the synoptic environments of the target years, of
230 precipitation processes, and of events. The output is from forecasts of the Weather Research
231 and Forecasting (WRF) Model (Skamarock et al., 2008) run under the Antarctic Mesoscale
232 Prediction System (AMPS) (Powers et al., 2003; 2012), a real-time NWP capability that
233 supports the weather forecasting for the United States Antarctic Program (USAP). The (U.S.)
234 National Center for Atmospheric Research (NCAR) has run AMPS since 2000 to produce
235 twice-daily forecasts covering Antarctica with model grids of varying resolutions. The AMPS
236 WRF forecasts have been stored in the AMPS Archive and used extensively in studies (e.g.
237 Monaghan et al., 2005; Schlosser et al., 2008; Seefeldt and Cassano, 2008; Schlosser et al.,
238 2008; Seefeldt and Cassano, 2012). For 2009 and 2010, the WRF output over the Dome C
239 region reflects a forecast domain with a horizontal grid spacing of 15 km, employing 44
240 vertical levels between the surface and 10 hPa. This 15-km grid was nested within a 45-km
241 grid covering the Southern Ocean, and Fig. 2 shows these domains.

242 Model output from AMPS has been verified through various means over the years. Multi-
243 year AMPS forecast evaluations have been conducted (Bromwich et al., 2005), and WRF's
244 ability for the Antarctic in particular has been confirmed (Bromwich et al., 2013). AMPS's
245 and WRF's Antarctic performance has also been documented in a number of case and process
246 studies (e.g. Bromwich et al., 2013; Nigro et al., 2011; 2012; Powers, 2007; Bromwich et al.,
247 2013). For model development within AMPS, verification for both warm and cold season
248 periods is performed prior to changes in model versions or configurations (Powers et al.,
249 2012). The reliability of AMPS WRF forecasts is also reflected in their demand from
250 international Antarctic operations and field campaign forecasting efforts (see e.g. Powers et
251 al., 2012). Lastly, similarly to how it is used here, AMPS output has been a key tool in

252 previous published studies of Antarctic precipitation related to ice core analyses (Schlosser et
253 al., 2008; 2010a; 2010b).

254 In this study the WRF output from the AMPS archive is used to study both the synoptic
255 patterns/general atmospheric circulation and the local conditions related to the precipitation
256 regimes and events in the years compared. The WRF forecasts provide reliable depictions of
257 conditions and their evolution.

258

259 **5 Results**

260 **5.1 Temperature and precipitation**

261 Figure 3a shows the mean monthly air temperature observed at the Dome C AWS for 2009
262 and 2010 as well as the mean of 1996-2014. The mean annual cycle exhibits the typical
263 coreless winter (van Loon, 1967) with a distinct temperature maximum in summer
264 (December/January), which has no counterpart in winter, where the months May to August
265 show relatively similar values. This is due to a combination of the local surface radiation
266 balance and warm air intrusions. During the first part of the polar night, with the lack of short-
267 wave radiation, an equilibrium of downwelling and upwelling longwave radiation is reached;
268 advection of relatively warm air from lower latitudes further reduces the possibility for
269 cooling. Thus the temperature does not decrease significantly after May (Schwerdtfeger 1984;
270 King and Turner, 1997; ~~Schwerdtfeger 1984~~).

271 While during the summer months little difference is seen between 2009 and 2010 the winter
272 months are strikingly different. The lowest mean July temperature of the station record occurs
273 in 2010 with a value of $-69.7\text{ }^{\circ}\text{C}$. This is the lowest monthly mean ever observed at Dome C,
274 $5.9\text{ }^{\circ}\text{C}$ lower than the average 1996-2014, corresponding to a deviation of 1.7σ , σ being the
275 standard deviation. In contrast, the highest July mean temperature is found in 2009; with a
276 value of $-54.9\text{ }^{\circ}\text{C}$, it was $8.9\text{ }^{\circ}\text{C}$ higher (corresponding to 2.5σ) than the long-term July mean
277 and the only July mean that exceeded $-60\text{ }^{\circ}\text{C}$. In Figure 3b, observed daily mean temperatures
278 and daily precipitation sums for the years 2009 and 2010 are displayed. Again, the differences
279 between the two years are most striking in winter. In 2009, the temperature variability is very
280 high, and several warming events with temperatures up to almost $-30\text{ }^{\circ}\text{C}$ can be seen.
281 Minimum temperatures are rarely lower than $-70\text{ }^{\circ}\text{C}$ whereas in 2010, minima are close to -80
282 $^{\circ}\text{C}$. The highest temperature in the winter of 2010 was only slightly above $-50\text{ }^{\circ}\text{C}$. The winter

283 2009 thus was not only a “coreless winter”, but had a “warm” core due to the high number of
284 warm air intrusions.

285 | A very high precipitation value of 1.36 ~~mm~~ mm was measured on 9 February 2010, followed
286 | by 0.67 mm on 10 February, both classified as diamond dust from the photographic crystal
287 | analysis. ~~stems from only one event around 9 February.~~ Considering the extremely low
288 | density of diamond dust, a diamond dust amount of more than 1mm/day at first, seemed to be
289 | unlikely. However, the model data do show a precipitation event connected to warm air
290 | advection from the north (see below) for this day, which would indicate the occurrence of
291 | snowfall rather than diamond dust. Most likely a mixture of crystal types was found during
292 | this event with the diamond dust on top of the snow crystals, which possibly led to the
293 | classification of the event as diamond dust. (Note that the crystal classification was carried out
294 | purely from photographs by an expert at the Avalanche Institute in Italy and that snow crystals
295 | are also comparatively small at the temperatures prevailing at Dome C). Also, it was found
296 | that increased amounts of diamond dust can prevail after snowfall events when humidity is
297 | still increased compared to the average, but not large enough to cause real snowfall. The
298 | precipitation totals for May to September are 12.0 mm w.e. for 2009 and 4.3 mm w.e. for
299 | 2010. Daily sums exceed 0.25 mm only three times in 2010, but 16 times in 2009. Usually,
300 | high daily precipitation amounts are associated with relative maxima in air temperature. In
301 | general, the winter of 2010 was cold and dry, whereas 2009 was relatively warm and moist
302 | compared to the long-term average.

303 | Figure 4a shows monthly precipitation amounts for 2009 and 2010, distinguishing between
304 | diamond dust, hoar frost, and snowfall; Figure 4b gives the relative frequencies of the three
305 | different observed types of precipitation for both years. Again, large differences between 2009
306 | and 2010 are found. While approximately half of the precipitation fell as snow in 2009, less
307 | than a quarter of the total precipitation stemmed from snowfall in 2010, when mostly diamond
308 | dust was observed. As seen before, the winter months of May to September exhibit the
309 | largest differences. In particular, the extremely “warm” July of 2009 brought high amounts of
310 | snowfall. The lowest amounts of precipitation are seen in austral summer 2009/2010, with no
311 | precipitation observed in November and only very small amounts in December and January.

312 | The total amount of precipitation measured on the raised platform is 16.5 mm w.e. for 2009
313 | and 13.4 mm w.e. for 2010, compared to the mean annual accumulation of 25 mm w.e.
314 | derived from firn core and stake measurements (Frezzotti et al., 2005). From the available
315 | data it cannot be determined whether the difference is due to snow removed from the

316 measuring platform by wind or sublimation or snow added to the snow surface at the stake
317 array by wind (blowing or drifting snow) or deposition (re-sublimation).

318

319 **5.2 Atmospheric flow conditions**

320 **5.2.1 Synoptic analyses with AMPS archive data**

321 The synoptic situations that caused precipitation at Dome C were analysed using WRF output
322 data from the AMPS archive. In particular, fields of 500hpa geopotential height and 24-h
323 precipitation were used. For the 500hPa geopotential height information the 12-h forecast was
324 utilized. For 24-h precipitation, the 12-36h forecast sums of precipitation (rather than 0-24h)
325 were used to allow for model spin up of clouds and microphysical fields. This is considered
326 long enough for moist process spin-up, but avoids error growth reflected in longer forecast
327 times (Bromwich et al., 2005).

328 For all precipitation events with observed daily sums exceeding 0.2mm, the synoptic
329 situations that caused the precipitation were investigated. In total, 29 events were studied, 20
330 in 2009 and 9 in 2010. For 2009 (2010), the model showed precipitation at Dome C in 44%
331 (50%) of the studied cases and precipitation in the vicinity in 33 (25) % of the cases; no
332 precipitation was shown in the model in 22 (25) % of the cases. In total, approximately half of
333 the precipitation events were represented well by the model, one quarter showed synoptic
334 events that did not bring precipitation exactly at the location and time of the measurements,
335 and one quarter of the cases were not forecast by the model at all. An exact quantitative
336 analysis of the model skill using the entire data series starting in 2006 is ongoing and the
337 results will be more meaningful than those of only two, not very typical, years.

338 Generally, snowfall events were found to be associated with an amplification of the Rossby
339 waves in the circumpolar westerlies, which causes a northerly flow across the Dome C region
340 between a trough to the west and an upper-level ridge to the east of Dome C. This northerly
341 flow brings relatively warm and moist air from as far as 35 °S - 40 °S to the East Antarctic
342 plateau, leading to orographic precipitation when it is forced to ascend on the way from the
343 coast to the high-altitude interior. Variations of this general situation are due to the duration of
344 the flow pattern (e.g. whether there is a blocking anticyclone or not) and the strength of the
345 upper-level ridge, which determines how far north the main moisture origin is situated. Figure
346 5 shows an example of this synoptic situation typical for snowfall events. In the 500hPa

347 geopotential height field (Fig. 5a) for 13 September 2009 the amplified ridge that leads to a
348 northerly flow towards Dome C can be seen slightly east of Dome C, with an axis tilted in a
349 NE-SW direction. Figure 5b displays the 24-h precipitation caused by the N-NE flow onto the
350 continent. Dome C is situated at the southeastern edge of the precipitation area.

351 A frequent occurrence of the synoptic situation described (as it was the case in 2009) means a
352 more northern mean moisture source than on average, which has to be taken into account for
353 deriving air temperature from stable isotopes. (A detailed study using trajectory calculations
354 for all observed precipitation events at Dome C is ongoing.) It was also found to be typical for
355 precipitation events at Dome C that the main westerly flow is split into a northern branch that
356 remains zonal, whereas the southern branch starts meandering with a strong meridional
357 component. This is observed more often at Dome C than at Dome F (Dittmann et al., 2015) or
358 at Kohnen Station (Schlosser et al., 2010a).

359 Figure 6 presents an example for a case with no precipitation in the model, but relatively large
360 observed precipitation amounts. The 500hPa geopotential height field (Fig. 6a) shows a
361 cutoff-high west of Dome C on the day after the precipitation event shown in Figure 5. The
362 remaining atmospheric moisture is not sufficient to produce precipitation in the model (Fig.
363 6b), but it does lead to remarkably high amounts of diamond dust and/or hoar frost (0.7 mm
364 observed during this event). This synoptic situation was also found by Hirasawa et al. (2013)
365 in a detailed study of the synoptic conditions and precipitation during and after a blocking
366 event at Dome Fuji. (Note that neither diamond dust nor hoar frost formation is specifically
367 parameterized in the model.) In 2010, the flow was mainly zonal and the synoptic situations
368 described above were much less frequent than in 2009 and not as strongly developed.

369 | Using the WRF output, monthly ~~composite-mean~~ fields of 500hPa-geopotential height were
370 calculated to compare the general flow conditions in 2009 and 2010. Figure 7 shows the
371 composite mean 500-hPa geopotential height for July 2009 and 2010, respectively. Even in
372 the monthly mean, the distinct upper-level ridge in 2009 that projects onto the East Antarctic
373 plateau and leads to warm air advection and increased precipitation at Dome C is clearly seen.

374 In 2010, in the monthly average, the flow was mainly zonal, which reduced the meridional
375 exchange of heat and moisture, thus leading to lower temperatures and less precipitation in the
376 interior of the Antarctic continent.

377

378 5.2.2 Southern Annular Mode

379 The occurrence of high-precipitation events on the Antarctic plateau due to amplification of
380 Rossby waves is often connected to a strongly positive phase of the Southern Annular Mode
381 (SAM). The SAM is the dominant mode of atmospheric variability in the extratropical
382 Southern Hemisphere. It is revealed as the leading empirical orthogonal function in many
383 atmospheric fields (e.g. Thompson and Wallace, 2000), such as surface pressure, geopotential
384 height, surface temperature, and zonal wind (Marshall, 2003). Since pressure fields from
385 global reanalyses commonly used to study the SAM are known to have relatively large errors
386 in the polar regions, Marshall (2003) defined a SAM index based on surface observations. He
387 calculated the pressure differences between 40 °S and 65 °S using data from six mid-latitude
388 stations and six Antarctic coastal stations to calculate the corresponding zonal means. A large
389 (small) meridional pressure gradient corresponds to a positive (negative) SAM index. The
390 positive index means strong, mostly zonal westerlies and comparatively little exchange of
391 moisture and energy between middle and high latitudes, which leads to a general cooling of
392 Antarctica, except for the Antarctic Peninsula that projects into the westerlies. A negative
393 SAM index is associated with weaker westerlies and a larger meridional flow component.

394 Figure 8 shows the monthly mean SAM index for 2009 and 2010 (data can be found at
395 <http://www.nerc-bas.ac.uk/icd/gjma/sam.html>). Whereas in the winter months (May to
396 September) of 2009 the SAM index was generally negative (with the exception of a weakly
397 positive value in June), 2010 has positive indices from April to August, with strongly positive
398 values in June and July, and only a weakly negative index in September. This is consistent
399 with the pattern of a strong zonal flow with few precipitation events at Dome C due to
400 amplified ridges in the winter of 2010, with the opposite situation holding in 2009. The
401 highest SAM index is found in November 2010; however, in austral summer the relationship
402 between the SAM index and precipitation seems to be less straightforward. The differences
403 between 2009 and 2010 are not extraordinarily high compared to other years (e.g. 2001/2002
404 as seen at <http://www.nerc-bas.ac.uk/public/icd/gjma/newsam.spr.pdf>), however, qualitatively
405 they are in agreement with the observed flow pattern. Furthermore, it should be kept in mind
406 that SAM explains only about one third of the atmospheric variability in the Southern
407 Hemisphere (Marshall, 2007) and that the SAM index alone gives no information about the
408 location of respective ridges and troughs in a highly meridional flow pattern.

409

410 5.2.3 Zonal wave number 3

411 Another method to investigate the general atmospheric flow conditions is to analyse spatial
412 and temporal variations of the quasi-stationary zonal waves in the Southern Hemisphere. In
413 this study zonal wave number 3 (ZW3) is used. While the atmospheric circulation in the
414 Southern Hemisphere appears strongly zonal (or symmetric), there is a significant non-zonal
415 (asymmetric) component and ZW3 represents a significant proportion of this asymmetry. It is
416 a dominant feature of the circulation on a number of different time scales (e.g. Karoly, 1989),
417 is responsible for 8% of the spatial variance in the field (van Loon and Jenne, 1972), and
418 contributes significantly to monthly and interannual circulation variability (e.g. ~~Trenberth,~~
419 ~~1990;~~Trenberth and Mo, 1985; ~~Trenberth, 1990~~). The asymmetry is revealed when the zonal
420 mean is subtracted from the geopotential height field thereby creating a coherent pattern of
421 zonal anomalies, with the flow associated with these patterns becoming apparent. ZW3 has
422 preferred regions of meridional flow, which influence the meridional transport of heat and
423 moisture into and out of the Antarctic. Raphael (2004) defined an index of ZW3 based on its
424 amplitude (effectively the size of the zonal anomaly) at 50°S showing that ZW3 has
425 identifiable positive and negative phases associated with the meridionality of the flow. A
426 positive value for this index indicates more meridional flow (large zonal anomaly) and a
427 negative value more zonal flow (small zonal anomaly). Note that the ZW3 index used here
428 does not fully capture the shift in phase of the wave. However, Raphael (2004) found that the
429 net effect is a small reduction in the amplitude of the wave, but the sign of the index is not
430 influenced. A new approach for identifying Southern Hemisphere quasi-stationary planetary
431 wave activity that allows variations of both wave phase and amplitude is described in a recent
432 study by Irving and Simmonds (2015).

433 Figure 9a shows the monthly mean ZW3 index for the period 2009–2010. From June to
434 September 2009 the ZW3 index was largely positive except for a comparatively small
435 negative excursion in July. On the contrary, from June to September 2010 it was negative. The
436 asymmetry in the circulation suggested by the index is shown in Figure 9b (July 2009) and 9c
437 (July 2010). These figures were created by subtracting the long-term zonal mean at each
438 latitude, from the mean 500-hPa geopotential height field in July 2009 and 2010, respectively.
439 The flow onto Dome C suggested by the alternating negative and positive anomalies is
440 northerly in July 2009, but has a strong zonal component in July 2010. This information given
441 by the ZW3 index and the patterns of zonal anomalies is consistent with that suggested by the
442 SAM.

443

444 **6 Discussion and Conclusion**

445 In the present study that was motivated by stable water isotope studies, atmospheric
446 conditions of the two contrasting years 2009 and 2010 at the Antarctic deep-drilling site
447 Dome C, on the East Antarctic Plateau were investigated using observational precipitation and
448 temperature data and data from a mesoscale atmospheric model. The observations from Dome
449 C represent the first and only multi-year series of daily precipitation/stable isotope
450 measurements at a deep-drilling site, even though “multi” means only nine years in this case.
451 The differences between the two years 2009 and 2010 were most striking in winter. Whereas
452 2009 was relatively warm and moist due to frequent warm air intrusions connected to
453 amplification of Rossby waves in the circumpolar westerlies, the winter of 2010 was
454 extremely cold and dry, with the lowest monthly mean July temperature observed since the
455 beginning of the AWS measurements in 1996. This can be explained by the prevailing strong
456 zonal flow in the winter of 2010, related to a strongly positive SAM index and a negative
457 ZW3 index. Also, the frequency distribution of the various precipitation types was largely
458 different in 2009 and 2010, with snowfall prevailing in 2009 whereas diamond dust was
459 dominant in 2010.

460 Similarly striking differences in weather conditions of 2009 and 2010 were seen in other parts
461 of East Antarctica. Gorodetskaya et al. (2013) found that accumulation in 2009 was eight
462 times higher than in 2010 at the Belgian year-round station “Princess Elisabeth”. At this
463 location, the temperature was also higher in 2009 than in 2010, particularly in fall/early
464 winter. The findings are supported by Boening et al. (2012), who used observations from
465 GRACE (Gravity Recovery And Climate Experiment) and found an abrupt mass increase on
466 the East Antarctic ice sheet in the period 2009-2011. Similarly, Lenaerts et al. (2013)
467 investigated snowfall anomalies in Dronning Maud Land, East Antarctica. They stated that the
468 large positive anomalies of accumulation found in 2009 and 2011 stand out in the past
469 approximately 60 years although comparable anomalies are found further back in time.

470 Distinguishing between the different forms of precipitation, namely diamond dust, hoar frost
471 and dynamically caused snowfall, is important for both mass balance and ice core
472 interpretation. For mass balance, the different precipitation types do not have to be known if
473 the surface mass balance is determined as an annual value from snow pits, firn/ice cores or
474 stake arrays. For temporally higher resolved precipitation measurements, however, a fraction

475 of both hoar frost and diamond dust might be just a part of the local cycle of sublimation and
476 deposition (re-sublimation), thus representing no total mass gain. More detailed
477 measurements are thus necessary to allow a better understanding of the processes involved.
478 This also applies to isotopic fractionation during this cycle; continuous measurements of
479 water vapour stable isotope ratios (e.g. Steen-Larsen et al., 2013) should be included here.

480 For ice core interpretation, the problem generally becomes more complex. Diamond dust is
481 observed during the entire year without a distinct seasonality. Therefore a signal from an ice
482 core property measured in the ice (in contrast to measured in the air bubbles) will have
483 contributions from diamond dust that stem nearly equally from all seasons. Although snowfall
484 events are not very frequent at deep ice core drilling sites, they can account for a large
485 percentage of the total annual precipitation/accumulation at those locations. If these events
486 have a seasonality that has changed between glacials and interglacials, a large bias will be
487 found in the temperature derived from the stable isotopes in ice cores. Today, the frequency of
488 such snowfall events shows a high inter-annual variability, but both frequency and seasonality
489 of the events might be different in a different climate due to changes in the general
490 atmospheric circulation and in sea ice extent (e.g. Godfred-Spenning and Simmonds, 1996).
491 Since it was found that snowfall events are connected to the synoptic activity in the
492 circumpolar trough, it is plausible that the seasonality of such events was different during
493 glacial times because the sea ice edge and the mean position of the westerlies were
494 considerably farther north than today. This influences the zone of the largest meridional
495 temperature gradient, thus the largest baroclinicity and consequently cyclogenesis. A larger
496 sea ice extent might reduce the number of snowfall events in the Antarctic interior in winter
497 by pushing the zone of largest baroclinicity northwards. However, it is not possible to assess
498 such hypotheses using observational data since the instrumental period, with few exceptions,
499 started in Antarctica not before the IGY (International Geophysical Year) 1957/58. However,
500 modelling studies can be supported by studies of the physical processes in the atmosphere
501 using recent data, and, in particular, cases of extreme situations can be helpful here. Even if
502 the full amplitude of the change between glacial and interglacial climates is not observed,
503 extrema can give insight into the sign and kind of the reaction of the system to a change in
504 one or several atmospheric variables.

505 Another implication for ice core interpretation derived from the present study is that a more
506 northern moisture source does not necessarily mean larger isotopic fractionation (which is
507 usually assumed in ice core studies (e.g. Stenni et al., 2001; 2010). Even without a

508 quantitative determination of the moisture source it can be said that in an increased meridional
509 flow, as in 2009, heat and moisture transport from relatively low latitudes is increased, too,
510 and leads to higher precipitation stemming from more northern oceanic sources than on
511 average. Although the temperature at the main moisture source is higher than on average for a
512 more northern moisture source, the depletion in heavy isotopes is comparatively small
513 because the temperature at the deposition site is also clearly higher than on average due to the
514 warm air advection, which reduces the temperature difference between the moisture source
515 region and the deposition site, thus the amount of isotopic fractionation.

516 Looking towards future work, the results here indicate that a combination of process studies
517 using recent data and modelling of the atmospheric flow conditions on larger time scales will
518 lead to a better quantitative interpretation of ice core data. Apart from the factors influencing
519 precipitation itself, it has become clear recently that post-depositional processes between
520 snowfall events are more important than previously thought because, additionally to processes
521 within the snowpack, the interaction between the uppermost parts of the snowpack and the
522 atmosphere is very intense (Steen-Larsen et al., 2013). Parallel measurements of stable
523 isotope ratios of water vapour and surface snow, combined with meteorological data will give
524 more insight into these processes in Antarctica.

525 Altogether, this means that, compared to years with predominantly zonal flow (which is the
526 more frequent situation), in years with enhanced meridional flow (negative SAM index,
527 positive ZW3 index) higher temperatures and higher amounts of precipitation that is less
528 depleted of heavy isotopes are expected at Dome C and comparable interior sites in
529 Antarctica. This is particularly valid for the colder seasons.

530 The relationship between air temperature and stable isotopes of Antarctic precipitation/ice is
531 anything else but straightforward, since the isotope ratio measured in an ice core (or in the
532 snow) is the result of a complex precipitation history that is strongly influenced by the
533 synoptics and general atmospheric flow conditions, followed by post-depositional processes.
534 Without thorough knowledge of all the processes involved a quantitatively correct derivation
535 of paleo temperatures from ice core stable water isotopes is thus not possible.

536

537 **Author contribution**

538 BS is responsible for the precipitation measurements, MV and AC for the crystal analysis.
539 MR did the ZW3 study. MD and KW assisted with software development. ES prepared the
540 manuscript with contributions from JP, KW, MR, and BS.

541

542

543 **Acknowledgements**

544 The precipitation measurements at Dome C have been conducted in the framework of the
545 Concordia station glaciology and ESF PolarCLIMATE HOLOCLIP projects funded in Italy
546 by PNRA-MIUR. This is a HOLOCIP publication number xx. The present study is financed
547 by the Austrian Science Funds (FWF) under grant P24223. AMPS is supported by the U.S.
548 National Science Foundation, Division of Polar Programs. We appreciate the support of the
549 University of Wisconsin-Madison Automatic Weather Station Program with the Dome C II
550 data set. (NSF grant numbers ANT-0944018 and ANT-12456663). We thank Gareth Marshall
551 for providing the SAM indices online. We thank all winterers at Dome C, who did the
552 precipitation sampling. We also thank our editor, Heini Wernli, and Harald Sodemann and
553 two anonymous reviewers for helpful comments that improved the manuscript.

554

555

556

557

558

559

560

561

562

563

564

565

566

567

568

569

570

571

572

573 **References**

574

575 Birnbaum, G., Brauner, R., and Ries, H.: Synoptic situations causing high precipitation rates
576 on the Antarctic plateau: observations from Kohnen Station, Dronning Maud Land , Antarctic
577 Science, 18 (2), pp. 279-288, doi: 10.1017/S0954102006000320, 2006.

578 Boening, C., Lebsack, M., Landerer, F., and Stephens, G. : Snowfall-driven mass change on
579 the East Antarctic ice sheet. Geophys. Res. Let., 39, L21501, doi:10.1029/GL053316, 2012.

580 Braaten, D. A.: Direct measurements of episodic snow accumulation on the Antarctic polar
581 plateau. J. Geophysic. Res., 105, (D9) 10,119-10,128, 2000.

582 Bromwich, D. H: Snowfall in high southern latitudes. Rev. Geophys., 26(1) 149-168, 1988.

583 Bromwich, D. H., Guo, Z., Bai, L., and Chen, Q. : Modeled Antarctic Precipitation. Part I:
584 Spatial and Temporal Variability, *J. Climate*, **17**, 427–447, 2004.

585 Bromwich, D. H., Monaghan, A. J., Manning, K. W., and Powers, J. G.: Real-time forecasting
586 for the Antarctic: An evaluation of the Antarctic Mesoscale Prediction System (AMPS), Mon.
587 Weather Rev., 133, 579-603, 2005.

588 Bromwich, D. H., Otieno, F. O., Hines, K. M., Manning, K. W., and Shilo, E.: Comprehensive
589 evaluation of polar weather research and forecasting performance in the Antarctic. J.
590 Geophys. Res., 118, 274–292, doi: 10.1029/2012JD018139, 2013.

591 Church, J.A., et al.: Sea Level Change. In: Climate Change 2013: The Physical Science Basis.
592 Contribution of Working Group I to the Fifth Assessment Report of the Intergovernmental
593 Panel on Climate Change (Stocker, T.F., D. Qin, D., G.K. Plattner, G. K., M. Tignor, M.,

594 Allen, S. K., Boschung, J., Nauels, A., Xia, Y., Bex, V., and Midgley, P. M. (eds.)),
595 Cambridge University Press, Cambridge, United Kingdom and New York, NY, USA, 2013.

596 Dansgaard, W.: Stable isotopes in precipitation, *Tellus*, XVI (4), 436-468, 1964.

597 Dittmann, A., Schlosser, E., Masson-Delmotte, V., Powers, J. G., Manning, K. W., Werner,
598 M., and Fujita, K.: Precipitation regime and stable isotopes at Dome Fuji, East Antarctica,
599 *Atmos. Chem. Phys. Discuss.*, doi:10.5194/acp-2015-1012, in review, 2016. Enomoto et al.,
600 Winter warming over Dome Fuji, East Antarctica and semiannual oscillation in the
601 atmospheric circulation. *J. Geophys. Res.*, 103 (D18), 23,103-23,111, 1998.

602 EPICA community members: 8 Glacial cycles from an Antarctic ice core, *Nature*, 429, 623-
603 628, doi:10.1038/nature02599, 2004.

604 Fogt, R. L. In: Arndt, D. S., Baringer, M. O., and M. R. Johnson, Eds., *State of the Climate in*
605 *2009*, 6. Antarctica. Special supplement to *Bull. Am. Meteorol. Soc.*, 91 (7) 125-134, 2010.

606 Fogt, R. L. In: Blunden, J., Arndt, D. S., Baringer, M. O., Eds., *State of the Climate in 2010*,
607 6. Antarctica. Special supplement to *Bull. Am. Meteorol. Soc.*, 92 (6) 161-172, 2011.

608 Frezzotti, M., Pourchet, M., Onelio, F., Gandolfi, S., Gay, M., Urbini, S., Vincent, C., Becagli,
609 S., Gragnani, R., Proposito, M., Severi, M., Traversi, R., Udisti, R., and Fily, M.: Spatial and
610 temporal variability of snow accumulation in East Antarctica from traverse data, *J. Glaciol.*,
611 51(178), 113-123, 2005.

612 Frieler, K., Clark, P. U., He, F., Buizert, C., Reese, R., Ligtenberg, S.R. M., Van den Broeke,
613 M. R., Winkelmann, R., and Levermann, A.: Consistent evidence of increasing Antarctic
614 accumulation with warming, *Nature Climate Change*, 5, 348-352,
615 doi:10.1038/NCLIMATE2574, 2015.

616 Fujita, K., and Abe, O.: Stable isotopes in daily precipitation at Dome Fuji, East Antarctica,
617 *Geophys. Res. Lett.*, 33, L18503, doi:10.1029/2006GL026936, 2006.

618 Godfred-Spenning, C. and Simmonds, I.: An analysis of Antarctic Sea-Ice and Extratropical
619 cyclone associations. *Int. J. Climat.*, 16, 1315-1332, 1996.

620 Gorodetskaya, I.V., N.P.M. Van Lipzig, M. R. Van den Broeke, A. Mangold, W. Boot, and C.
621 H. Reijmer: Meteorological regimes and accumulation patterns at Utsteinen, Dronning Maud
622 Land, East Antarctica: Analysis of two contrasting years. *J. Geophys. Res.*, 118, 1-16,
623 doi:10.1002/jgrd.50177, 2013.

624 Harig, C., and Simons, F. J.: Accelerated West Antarctic ice mass loss continues to outpace
625 East Antarctic gains. *Earth Planet. Sci. Let.* 415, 134-141, doi:10.1016/j.epsl.2015.01.029,
626 2015.

627 Hirasawa, N., Nakamura, H., and Yamanouchi, T.: Abrupt changes in meteorological
628 conditions observed at an inland Antarctic station in association with wintertime blocking.
629 *Geophys. Res. Let.*, 27(13), 1911-1914, 2000.

630 Hirasawa, N., Nakamura, H., Motoyama, H., Hayashi, M., and Yamanouchi, T.: The role of
631 synoptic-scale features and advection in a prolonged warming and generation of different
632 forms of precipitation at dome Fuji station, Antarctica, following a prominent blocking event,
633 *J. Geophys. Res.*, 118, 6916-6928, doi:10.1002/jgrd.50532, 2013.

634 Jouzel, J., Vimeux, F., Caillon, N., Delaygue, G., Hoffmann, G., Masson-Delmotte, V., and
635 Parrenin, F.: Magnitude of isotope/temperature scaling for interpretation of central Antarctic
636 ice cores, *J. Geophysic. Res.*, 108 (D12), 4361, doi:10.1029/2002JD002677, 2003.

637 Jouzel, J., in: Heinrich Holland and Karl Turekian (Ed.) *Treatise on Geochemistry* (Second
638 Edition) 5.8, Elsevier, 213-256, 2014.

639 Karoly, D. J.: Southern Hemisphere circulation features associated with El Nino-Southern
640 Oscillation events, *J. Clim.*, 2, 1239-1251, 1989.

641 King, J. and Turner, J.: *Antarctic Meteorology and Climatology*. Cambridge Atmospheric and
642 Space Sciences Series, Cambridge University Press, Cambridge, 409pp, 1997.

643 Lenaerts, J. T. M., van Meijgaard, E., Van den Broeke, M.R., Ligtenberg, S. R. M., Horwarth,
644 M., and Isaksson, E.: Recent snowfall anomalies in Dronning Maud Land, East Antarctica, in
645 a historical and future climate perspective. *Geophys. Res. Let.*, 40, 2684-2688,
646 doi:10.1002/grl.50559, 2013.

647 Lorius, C., Merlivat, L., Jouzel, J., and Pourchet, M.: A 30,000 years isotope climatic record
648 from Antarctic ice, *Nature*, 280, (5724), 644-647, 1979.

649 Marshall, G. J.: Trends in the Southern Annular Mode from observations and reanalyses, *J.*
650 *Clim.*, 16, 4134-4143, 2003.

651 Marshall, G. J., : Half-century seasonal relationship between the Southern Annular Mode and
652 Antarctic temperatures, *Int. J. Climatol.*, 27, 373-383, 2007.

653 Massom, R., Pook, M. J., Comiso, J. C., Adams, N., Turner, J., Lachlan-Cope, T., and Gibson,
654 T.: Precipitation over the interior East Antarctic ice sheet related to midlatitude blocking-high
655 activity. *J. Climate*, 17, 1914-1928, 2004.

656 [Masson-Delmotte, V., H. Shugui, A. Ekaykin, J. Jouzel, A. Aristarain, R.T. Bernardo, D. H.](#)
657 [Bromwich, O. Cattani, M. Delmotte, S. Falourd, M. Frezotti, H. Gallée, L. Genoni, A.](#)
658 [Landais, M. Helsen, G. Hoffmann, V. Morgan, H. Motoyama, D. Noone, H. Oerter, J.R.Petit,](#)
659 [A.Royer, R. Ruemura, G. Schmidt, E. Schlosser, J. Simoes, E. Steig, B.Stenni, M. Stievenard,](#)
660 [F. Vimeux, J.W.C. White, 2008. A review of Antarctic surface snow isotopic composition:](#)
661 [observations, atmospheric circulation and isotopic modelling. *J. Climate*, 21\(13\), 3359-3387.](#)
662 [doi 10.1175/2007JCLI2139.1.](#)

663 Monaghan, A. J., Bromwich, D. H., Powers, J. G., Manning, K. W.: The Climate of
664 McMurdo, Antarctica, Region as Represented by One Year of Forecasts from the Antarctic
665 Mesoscale Prediction System, *J. Climate*, 18, 1174-1189, 2005.

666 Monaghan, A. J., Bromwich, D. H., Fogt, R. L., Wang, S., Mayewski, P. A., Dixon, D. A.,
667 Ekaykin, A., Frezzotti, M., Goodwin, I., Isaksson, E., Kaspari, S. D., Morgan, V. I., Oeter, H.,
668 Van Ommen, T. D., Van der Veen, C. J., and Wen, J.: Insignificant change in Antarctic
669 snowfall since the International Geophysical Year. *Science*, 313, 827-831, doi:
670 10.1126/science.1128243, 2006.

671 Nicolas, J. P. and Bromwich, D. H.: Climate of West Antarctica and Influence of Marine Air
672 Intrusions. *J. Climate*, 24, 49-67. doi:10.1175/2010JCLI3522.1, 2011.

673 Nigro, M. A., Cassano, J. J., and Seefeldt, M. W.: A weather pattern-based approach to
674 evaluate the Antarctic Mesoscale Prediction System (AMPS) forecasts: Comparison to
675 automatic weather station observations. *Wea. Forecasting*, 26, 184-198,
676 doi:10.1175/2010WAF2222444.1, 2011.

677 Nigro, M. A., Cassano, J. J., and Knuth, S. L.: Evaluation of Antarctic Mesoscale Prediction
678 System (AMPS) cyclone forecasts using infrared satellite imagery. *Antarctic Science*, 24, 183-
679 192, doi:10.1017/S0954102011000745, 2012.

680 Noone, D., and Simmonds, I.: Implications for the interpretation of ice-core isotope data from
681 analysis of modelled Antarctic precipitation. *Ann. Glaciol.*, 27, 398-402, 1998.

Formatiert: Schriftart: (Standard)
Times New Roman, 12 Pt.

682 Noone, D., and Simmonds, I.: Associations between $\delta^{18}\text{O}$ Of water and climate parameters in
683 a simulation of atmospheric circulation for 1979-95. *J. Clim.*, 15, 3150-3169, 2002.

684 Noone, D., Turner, J., and Mulvaney, R.: Atmospheric signals and characteristics of
685 accumulation in Dronning Maud Land, Antarctica. *J. Geophysic. Res.*, 104 (D16), 19,191-
686 19,211, 1999.

687 Nygard, T., Valkonen, T., and Vihma, T.: Antarctic Low-Tropopause Humidity Inversions: 10-
688 yr Climatology, *J. Climate*, 26, 5205-5219, doi: 10.1175/JCLI-D-12-00446.1, 2013.

689 Powers, J. G., Monaghan, A. J, Cayette, A. M., Bromwich, D. H., Kuo, Y., and Manning, K.
690 W.: Real-time mesoscale modeling over Antarctica. The Antarctic Mesoscale Prediction
691 System. *Bull. Am. Meteorol. Soc.*, 84, 1522-1545, 2003.

692 Powers, J. G.: Numerical prediction of an Antarctic severe wind event with the Weather
693 Research and Forecasting (WRF) Model. *Mon. Wea. Rev.*, 135, 3134-3157, 2007.

694 Powers, J. G., Manning, K. W., Bromwich, D. H., Cassano, J. J., and Cayette, A. M.: A decade
695 of Antarctic science support through AMPS. *Bull. Amer. Meteor. Soc.*, 93, 1699-1712, 2012.

696 Raphael, M. N.: A zonal wave 3 index for the Southern Hemisphere, *Geophys. Res. Let.*,
697 31(23), doi:10.1029/2004GL020365, 2004.

698 Reijmer C. H, Van den Broeke, M. R., and Scheele, M. P.: Air parcel trajectories and snowfall
699 related to five deep drilling locations in Antarctica based on the ERA-15 dataset, *J. Climate*,
700 15:1957–1968, 2002.

701 Reijmer, C. H. and van den Broeke, M. R.: Temporal and spatial variability of the surface
702 mass balance in Dronning Maud Land, Antarctica. *J. Glaciol.*, 49(167), 512-520, 2003.

703 Ritter, F., Steen-Larsen, H. C., Kipfstuhl, J., Orsi, A., Behrens, M., and Masson-Delmotte, V.:
704 First continuous measurements of water vapor isotopes on the Antarctic Plateau, *Geophys.*
705 *Res. Abstr.*, 16, EGU2014-9721, 2014.

706 Scarchilli, C., Frezzotti, M., and Ruti, P. M.: Snow precipitation at four ice core sites in East
707 Antarctica - provenance, seasonality and blocking factors. *Clim. Dyn.*, 37, 2107-2125,
708 doi:10.1007/s00382-010-0946-4, 2010.

709 Schlosser, E.: Effects of seasonal variability of accumulation on yearly mean $\delta^{18}\text{O}$ values in
710 Antarctic snow, *J. Glaciol.* , 45 (151), 463-468, 1999.

711 Schlosser, E., Duda, M. G., Powers, J. G., Manning, K. W.: The precipitation regime of
712 Dronning Maud Land, Antarctica, derived from AMPS (Antarctic Mesoscale Prediction
713 System) Archive Data. *J. Geophys. Res.*, 113, D24108, doi: 10.1029/2008JD009968, 2008.

714 Schlosser, E., K. W. Manning, K. W., Powers, J. G., Duda, M. G., Birnbaum, G., and Fujita,
715 K.: Characteristics of high-precipitation events in Dronning Maud Land, Antarctica. *J.*
716 *Geophys. Res.*, 115, D14107, doi:10.1029/2009JD013410, 2010.

717 Schlosser, E., Powers, J. G., Duda, M. G., Manning, K. W., Reijmer, C.H., Van den Broeke,
718 M.: An extreme precipitation event in Dronning Maud Land, Antarctica - a case study using
719 AMPS (Antarctic Mesoscale Prediction System) archive data. *Polar Research*,
720 doi:10.1111/j.1751-8369.2010.00164.x, 2010.

721 Schlosser, E., Manning, K. W., Powers, J. G., Gillmeier, S., and Duda, M. G., An extreme
722 precipitation/warming event in Antarctica – a study with Polar WRF, in preparation, 2016.

723 Sodemann, H, and A Stohl. 2009. Asymmetries in the moisture origin of Antarctic
724 precipitation. *Geophys.Res. Letters* 36: L22803. doi:10.1029/2009GL040242.
725

726 Sodemann, H., Masson-Delmotte, V., Schwierz, C., Vinther, B. M. and Wernli, H.: Inter-
727 annual variability of Greenland winter precipitation sources. Part II: Effects of North Atlantic
728 Oscillation variability on stable isotopes in precipitation, *J. Geophys. Res.*, 113, D12111,
729 doi:10.1029/2007JD009416, 2008.

730 Schwerdtfeger, W.: *Weather and Climate of the Antarctic*. Elsevier Science Publishers,
731 Amsterdam-London-New York-Tokyo. 262pp, 1984.

732 Seefeldt, M. W., and Cassano, J. J.: An analysis of low-level jets in the greater Ross Ice Shelf
733 region based on numerical simulations. *Mon. Wea. Rev.*, **136**, 4188-4205. doi:
734 10.1175/2007JAMC1442.1, 2008.

735 Seefeldt, M. W., and Cassano, J. J.: A description of the Ross Ice Shelf air stream (RAS)
736 through the use of self-organizing maps (SOMs). *J. Geophys. Res.*, **117**, D09112.
737 doi:10.1029/2011JD016857, 2012.

738 Simmonds, I., Keay, K., and Lim, E.: Synoptic activity in the seas around Antarctica. *Mon.*
739 *Wea. Rev.*, 131, 272-288, 2002.

740 Sinclair, M. R.: Record-high temperatures in the Antarctic – A synoptic case study, *Mon. Wea.*
741 *Rev.*, 109, 2234- 2242, 1981.

742 Skamarock, W. C., Klemp, J. B., Dudhia, J., Gill, D. O., Barker, D. M., Duda, M. G., Huang,
743 X., Wang, W, and Powers, J. G.: A description of the Advanced Research WRF Version 3,
744 NCAR/TN 475+STR, 125 pp., Nat. Cent. for Atmos. Res., Boulder, Co, 2008.

745 Stenni, B., Masson-Delmotte, V., Johnsen, S., Jouzel, J., Longinelli, A., Monnin, E.,
746 Roethlisberger, R., and Selmo, E.: An Oceanic Cold Reversal During the Last Deglaciation,
747 *Science*, 293, 2074-2077, 2001.

748 Stenni, B., Masson-Delmotte, V., Selmo, E., Oerter, H., Meyer, H., Roethlisberger, R., Jouzel,
749 J., Cattani, O., Falourd, S., Fischer, H., Hoffmann, G., Iacumin, P., Johnsen, S. F., Minster, B.,
750 and Udisti, R.: The deuterium excess records of EPICA Dome C and Dronning Maud Land
751 ice cores (East Antarctica), *Quat. Scie. Rev.*, 29, 146-159, 2010.

752 Steen-Larsen, H. C. , S. J. Johnson, S. J., Masson-Delmotte, V., Stenni, B., Risi, C.,
753 Sodemann, H., Balslev-Clausen, D., Blunier, T., Dahl-Jensen, D., Ellehøy, M. D., Falourd, S.,
754 Grindsted, A., Gkinis, V., Jouzel, J., Popp, T., Sheldon, S., Simonsen, S. B., Sjolte, J.,
755 Steffensen, J. P., Sperlich, P., Sveinbjörnsdottir, A. E., Vinther, B. M., White, J. W. C.:
756 Continuous monitoring of summer surface water vapor isotopic composition above the
757 Greenland Ice Sheet, *Atmos. Chem. Phys.*, 13, 4815-4828, 2013.

758 Suzuki, K., Yamanouchi, T., and Motoyama, H.: Moisture transport to Syowa and Dome Fuji
759 stations in Antarctica, *J. Geophys. Res.*, 113, D24 114, doi:10.1029/2008JD009794, 2008.

760 Thompson, D. W. J., and J. M. Wallace: Annular modes in the extratropical circulation. Part I:
761 Month-to-month variability, *J. Climate*, 13, 1000-1016.

762 Trenberth, K. E., and Mo, K. C.: Blocking in the Southern Hemisphere, *Mon. Weather Rev.*,
763 133, 38-53, 1985.

764 Van Loon, H.: The half-yearly oscillation in middle and high southern latitudes and the
765 coreless winter. *J. Atmos. Sci.*, 24, 472-486, 1967.

766 Van Loon, H., and Jenne, R. L., The zonal harmonic standing waves in the Southern
767 Hemisphere, *J. Geophys. Res.*, 77, 992-1003, 1972.

768 Winkelmann, R., Levermann, A., Martin, M. A., and Frieler, K.: Increased future ice
769 discharge from Antarctica owing to higher snowfall. *Nature*, 492, 239-242, 2012.

770

771

772

773

774

775

776

777 **Figure Captions**

778

779 **Fig. 1**

780 Map of Antarctica indicating Dome C and other important deep-drilling sites in Antarctica

781

782 **Fig. 2**

783 AMPS domains used for model output analysis in this study

784

785 **Fig. 3**

786 a) Mean monthly temperatures for 2009 and 2010 at Dome C AWS

787 b) Daily precipitation and daily mean temperature at Dome C for 2009 and 2010

788

789 **Fig. 4**

790 Monthly precipitation at Dome C a) 2009 and b) 2010, distinguishing three different types of
791 precipitation: diamond dust, hoar frost, and snowfall

792 Relative frequency of diamond dust, hoar frost, and snowfall for c) 2009 and d) 2010

793 The types were determined from photos of the crystals on the platforms by the Avalanche
794 Research Institute, Arabba, Italy.

795

796 **Fig. 5**

797 a) 500hPa geopotential height from AMPS archive data (Domain 1) 13.9.2009 00Z

798 (The axis of the upper-level ridge mentioned in the text is marked by a bold black line.)

799 b) 24h-precipitation from AMPS 13.9. 2009 00GMT to 24 GMT

800

801 **Fig. 6**

802 Example for synoptic situation, during which precipitation is observed at Dome C, but not
803 forecast by WRF in AMPS.

804 a) 500 hPa geopotential height, Domain 2.

805 b) 24h-precipitation total (mm) from AMPS

806

807 **Fig. 7**

808 Mean July- 500hPa geopotential height based on AMPS archive model output for 2009 and
809 2010.

810

811 **Fig. 8**

812 Mean monthly SAM index for 2009 and 2010 (after Marshall, 2003).

813

814 **Fig. 9**

815 a) Monthly mean Zonal Wave Number 3 (ZW3) index for 2009-2010

816 b) July 2009 500hPa geopotential height anomaly: Mean July 2009 height minus long-term
817 zonal mean height

818 c) July 2010 500hPa geopotential height anomaly: Mean July 2009 height minus long-term
819 zonal mean height

820

821

822

823

824

825

826 **Fig. 1**

827

828

829

830

831

832

833

834

835

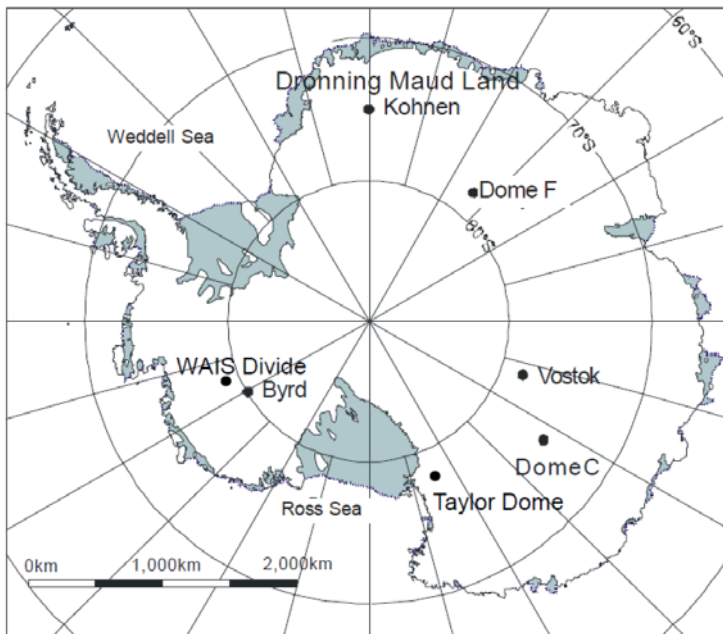
836

837

838

839

840



841

842

843

844

845

846

847

848

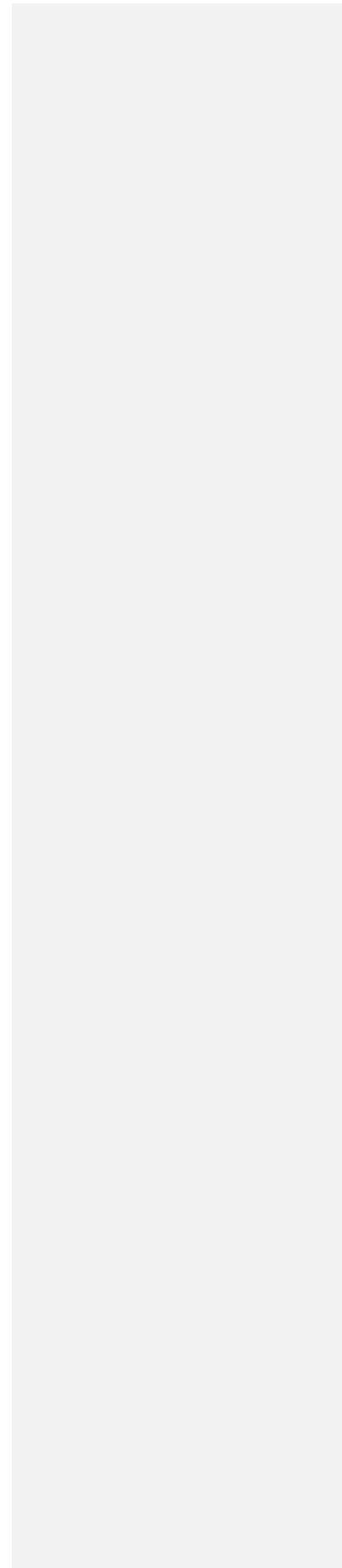
849

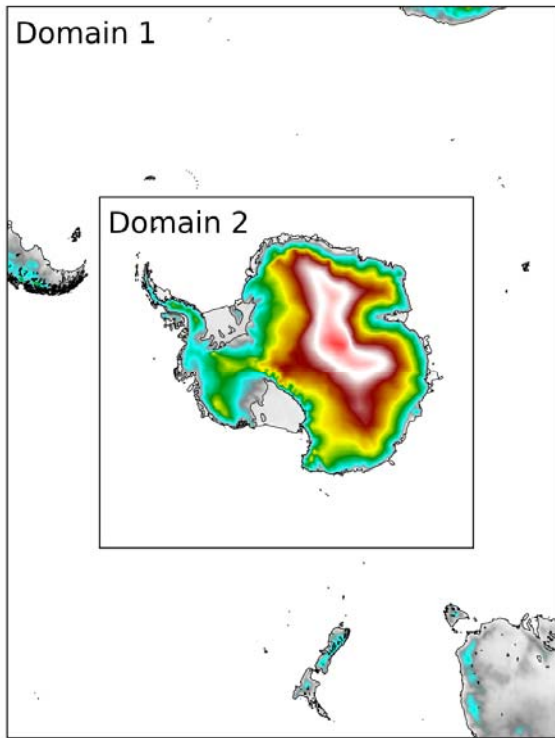
850

851

852 **Fig. 2**

853





854

855

856

857

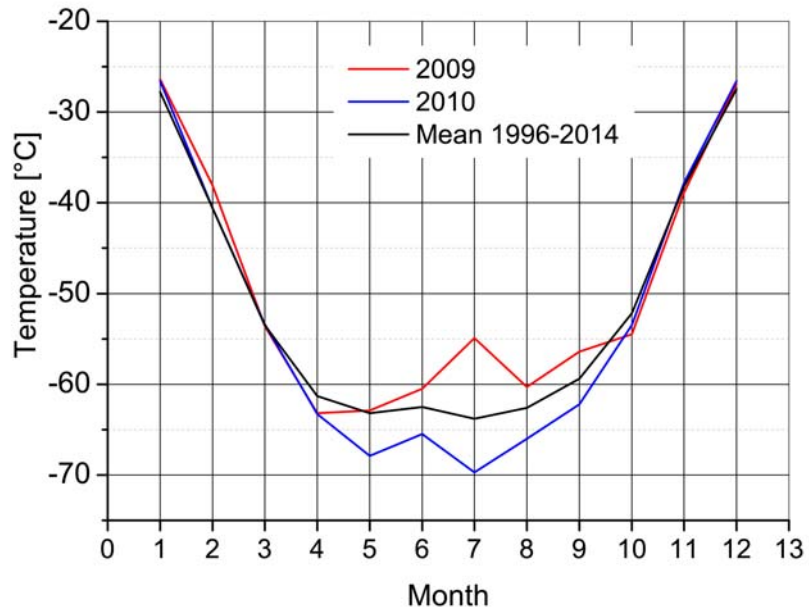
858

859

860 **Fig. 3**

861

862 a)



863

864

865

866

867

868

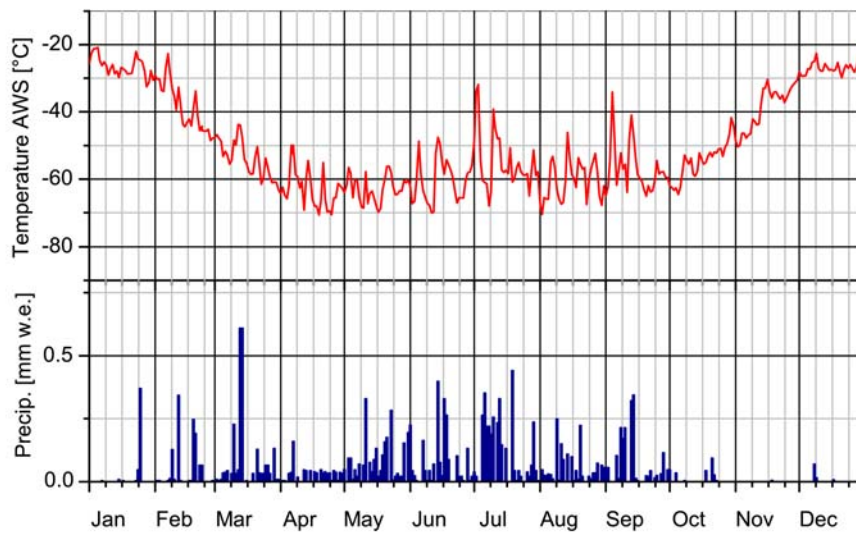
869

870

871

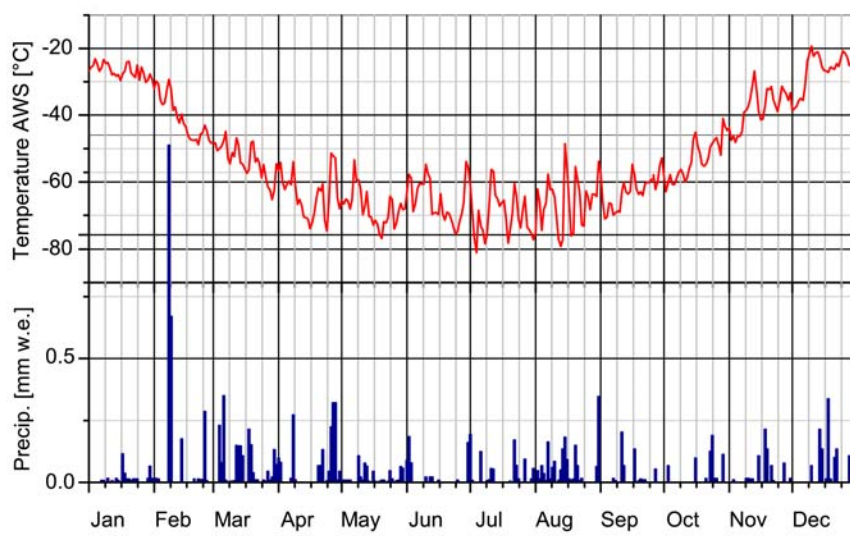
872 b)

873 2009



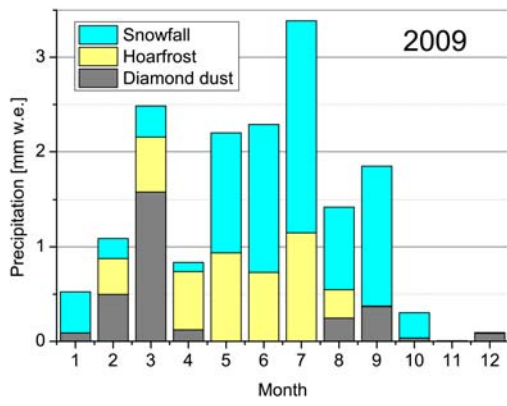
874 2010

875

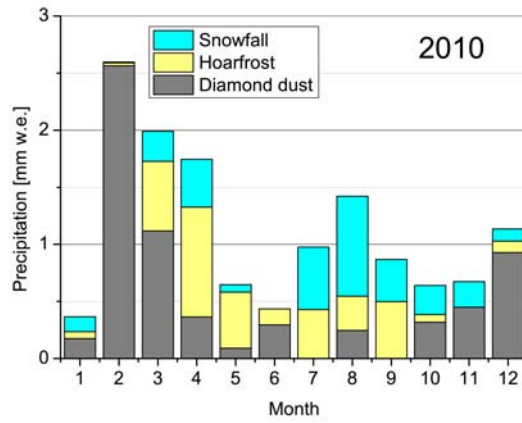


876 Fig. 4

877 a)



b)



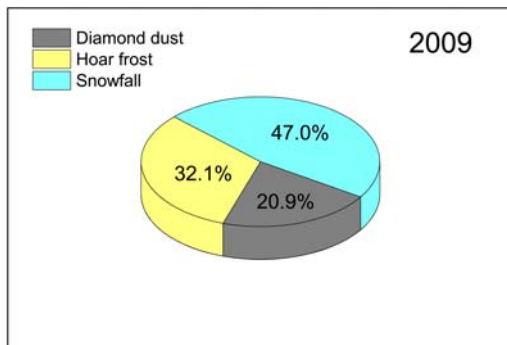
878

879

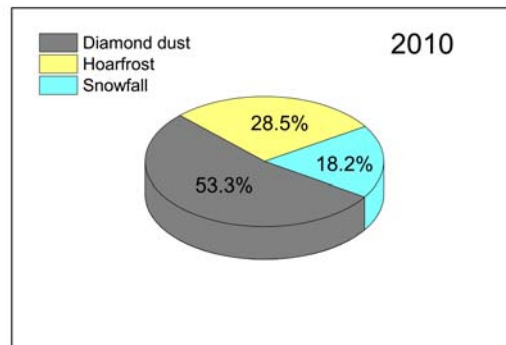
880 c)

881

882



d)



883

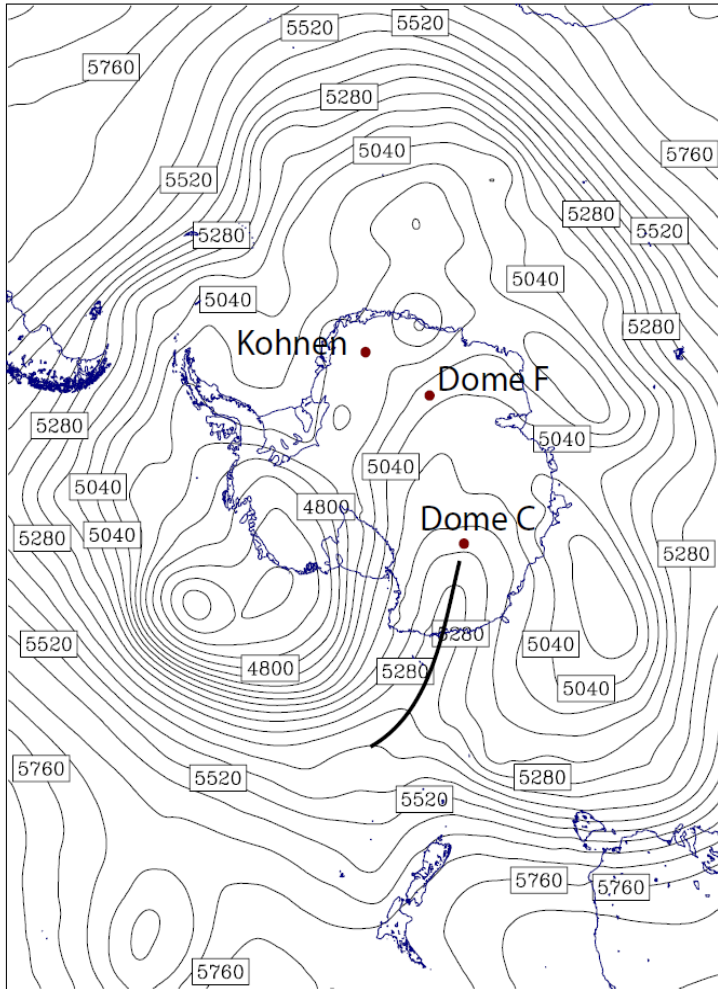
884

885

886 Fig. 5

887 a)

888



904

905

906

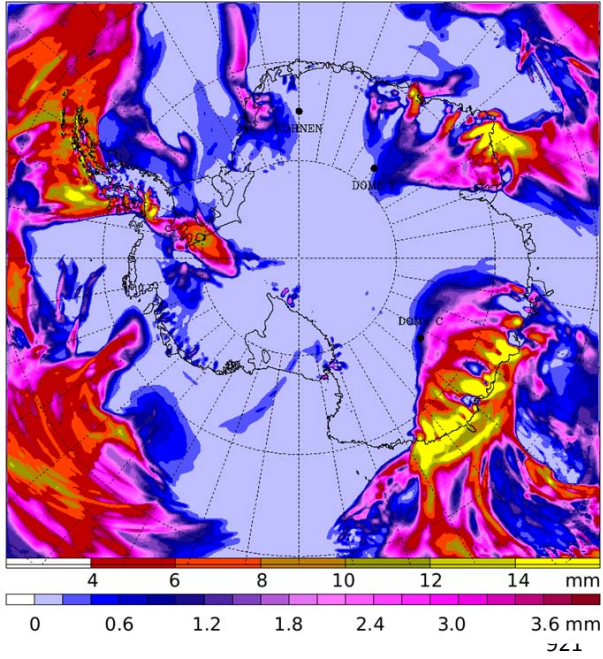
907

908

909

910 **b)**

911



922

923

924

925

926

927

928

929

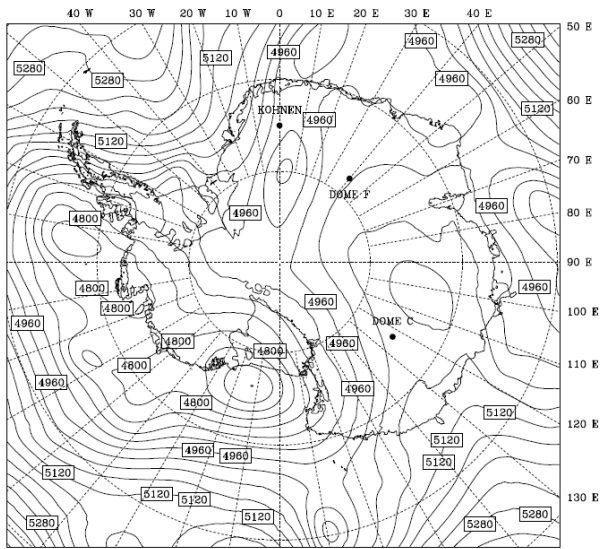
930

931

932 **Fig. 6**

933 **a)**

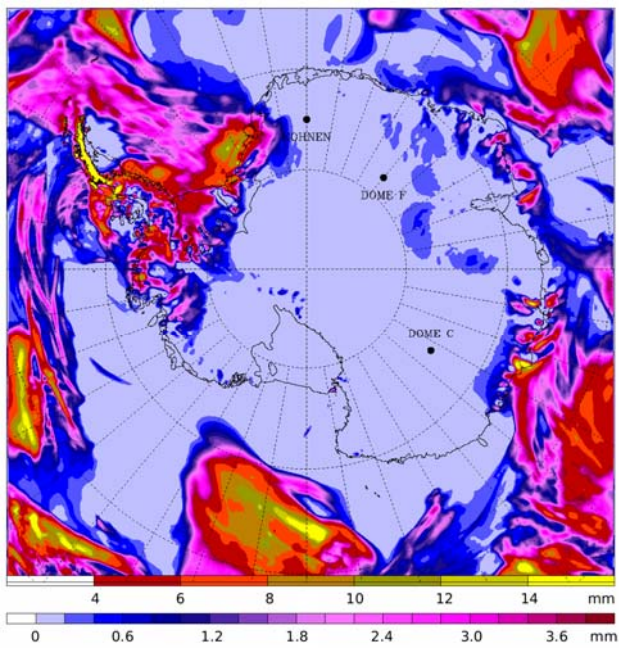
934



944

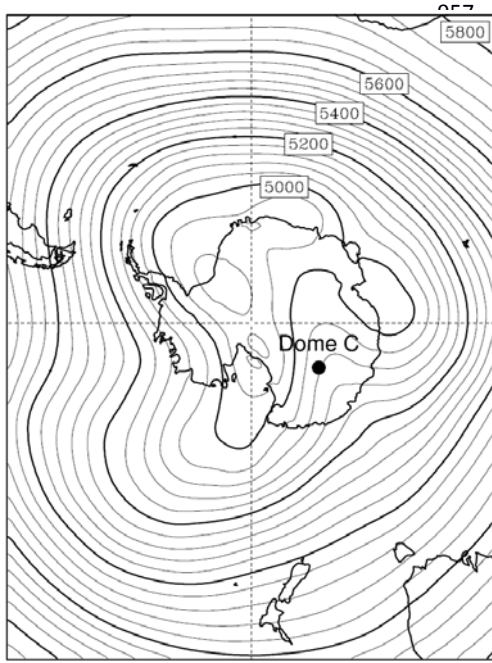
945 **b)**

946

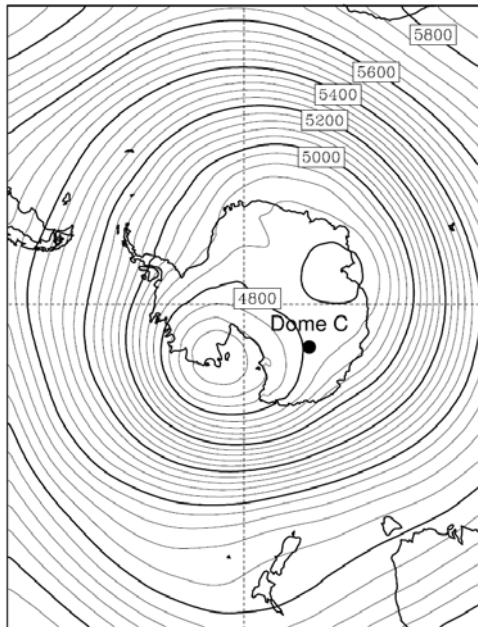


955 **Fig. 7**

956 a) July 2009



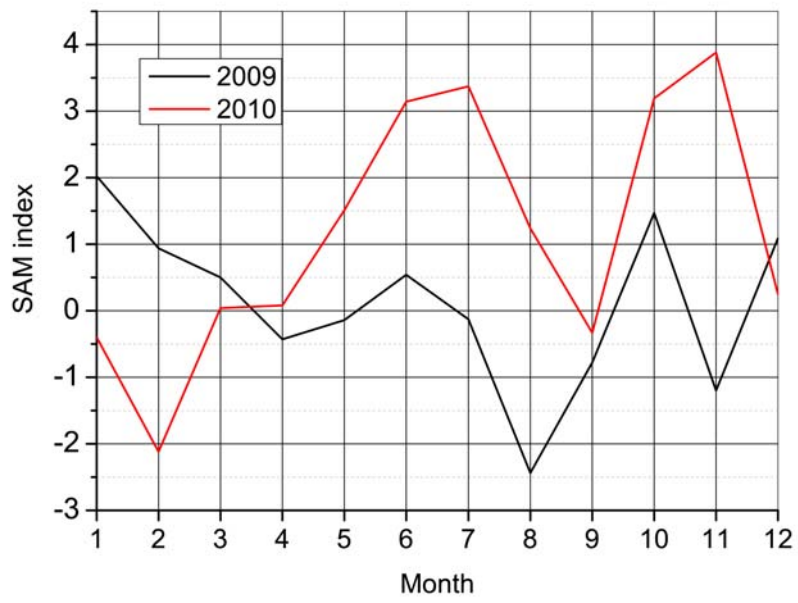
967 b) July 2010



978 **Fig. 8**

979

980



981

982

983

984

985

986

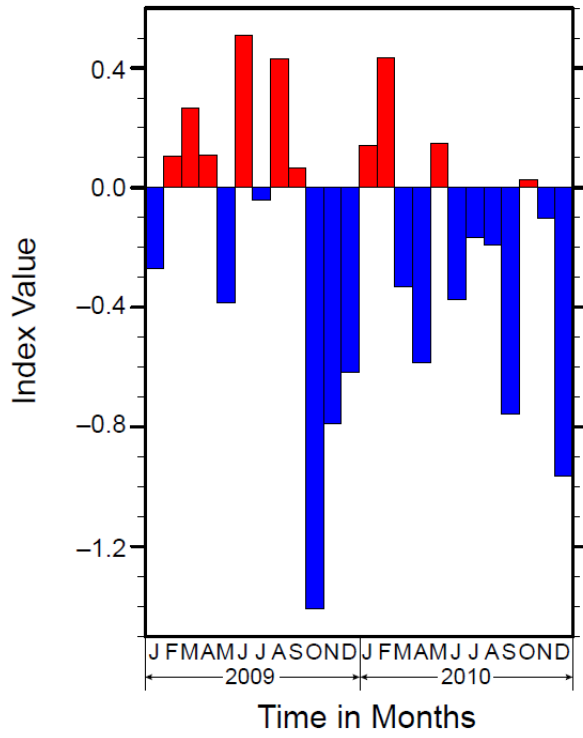
987

988

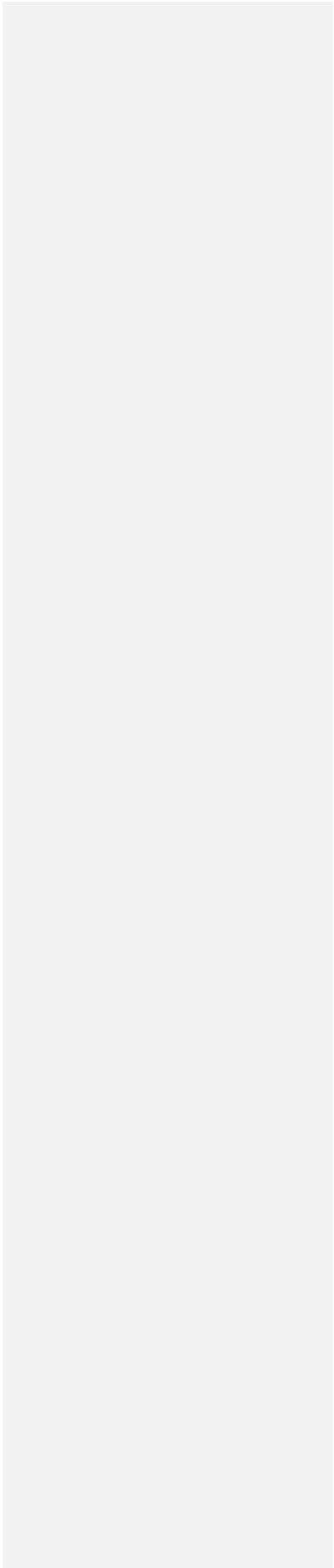
989

990 **Fig. 9**

991 a)

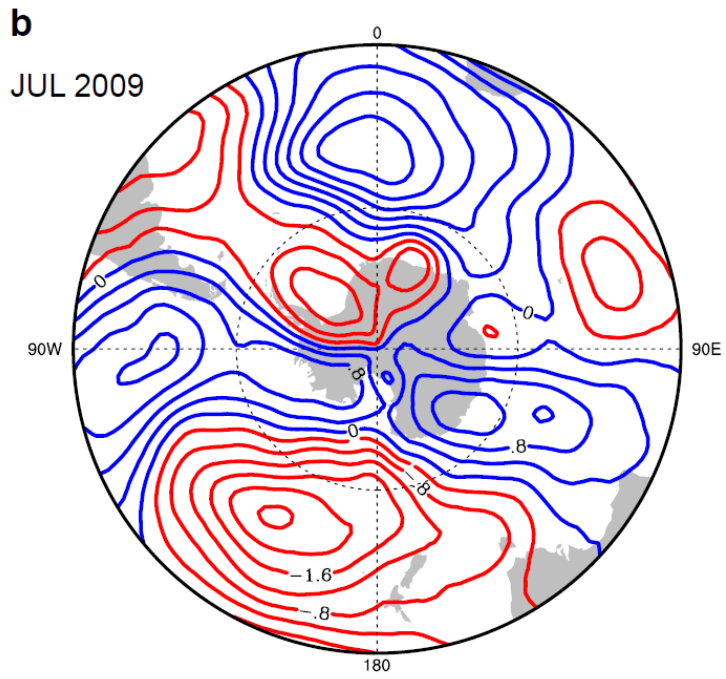


1003
1004
1005
1006
1007
1008
1009
1010
1011
1012



1013 b) 500hPa geopotential height: mean July 2009 minus long-term zonal mean

1014



1025 c) 500hPa geopotential height: mean July 2010 minus long-term zonal mean

1026

